

## Investigating the Spatial Resolution and Contrast of Peeled-Off Gafchromic EBT2 Film Exposed to 5 MeV Alpha Particles Analyzed via Color Channels

M. S. Ghaith<sup>1,2,\*</sup>, Nermeen A Kelany<sup>1</sup>, Manar A Ibrahim<sup>1</sup>, M. El Ghazaly<sup>1</sup>

<sup>1</sup>Department of Physics, Faculty of Science, Zagazig University, Zagazig 44519, Egypt

<sup>2</sup>Department of Basic Science, Faculty of Engineering, Sinai University – Kantara Branch, Ismailia 41636, Egypt.

\*Corresponding author: mohamed.diab1511998@yahoo.com

**ABSTRACT:** The relationship between spatial resolution and contrast of peeled-off EBT2 Radiochromic film irradiated with monoenergetic alpha particles across various color channels has been investigated. Gafchromic EBT2 films, after removing their protective layer, were checked for homogeneity, and then they were exposed to 5 MeV alpha particles from <sup>241</sup>Am source with various doses. A razor blade was used to create two distinct edges. The relation between the pixel values and contrast for different doses was studied. The edge spread function (ESF) data was fitted using the error function and then differentiated to derive the line spread function (LSF). All the channels except the blue one consistently exhibit a step transition between exposed and unexposed regions. In contrast, the blue channel displayed an irregular response, where the exposed area appeared unexpectedly brighter than the unexposed area, indicating limited sensitivity to alpha particle exposure. The average spatial resolution, expressed as the full width at half maximum (FWHM), was calculated to be  $(31 \pm 6.7) \mu\text{m}$ ,  $(25.6 \pm 3.4) \mu\text{m}$ ,  $(26.7 \pm 3.1) \mu\text{m}$ , and  $(23.8 \pm 3.3) \mu\text{m}$  for the red and green channels, as well as the weighted and unweighted gray images, respectively, indicating that the unweighted gray image and the green channel provide the highest spatial resolution.

**KEYWORDS:** Peeled-off Gafchromic EBT2 film, alpha particles, color channels, flatbed scanner, edge-and-line spread function.

Date of Submission: 25-01-2025

Date of acceptance: 10-04-2025

### I. INTRODUCTION

Radiochromic films serve as two-dimensional dosimeters that involve direct coloration when exposed to radiation. These films are used in different clinical applications, such as dose mapping for X-rays, gamma rays, beta particles, and heavy ion radiotherapy [1, 2]. These films present numerous specifications for dosimetry in clinical settings, such as their near-tissue equivalence, self-developing characteristics, low energy dependence, and high spatial resolution [3]. The responsible for the color change in radiochromic films are identified as crystalline polyacetylenes, specifically diacetylenes [4].

Advanced radiotherapy techniques like Intensity-modulated radiotherapy (IMRT) or stereotactic radiosurgery (SRS) deliver highly conformal doses to a specific target volume. Accurate spatial resolution ensures that these complex localized dose distributions are captured and reproduced precisely, reducing the risks of underdosing tumors or overdosing healthy tissue [5, 6]. Poor spatial resolution can result in blurring, deformation, or loss of key dose distribution details, potentially affecting treatment outcomes [3].

The most used family of radiochromic films is the external beam therapy (EBT) Gafchromic films, which are extensively utilized in clinical applications for precise radiation dose mapping [7]. The active layer of the Gafchromic EBT2 film, which has an effective atomic number ( $Z_{\text{eff}}$ ) of 6.84, closely approximating human tissue, has been modified for uniformity by adding a yellow marker dye [8]. The response of the Gafchromic EBT2 film to various doses is primarily compared with the absorbed dose of the incident radiation. However, it remains independent of the fluence or energy of the incident radiation [9]. The digitizing system and high spatial resolution of these films are crucial for precise radiation dose mapping. In principle, higher spatial resolution correlates with greater accuracy in the radiation dose delivered to malignant tumors. This is particularly significant in the context of both high and low-heavy-ion radiotherapy [10, 11]. Spatial resolution in dose

mapping indicates the ability of a system or medium to precisely distinguish and represent variations in radiation dose across different regions of a target area. Spatial resolution is typically measured in units like micrometers ( $\mu\text{m}$ ) or dots per inch (DPI), indicating the smallest detectable detail or change in dose distribution that the system can accurately record and display [3, 12].

Many types of radiochromic films differ in construction and materials composition [1, 6]. In this study, our focus is on one specific type: EBT2 Gafchromic film. The construction of EBT2 film consists of a 30  $\mu\text{m}$  active layer, 5  $\mu\text{m}$  top coat, 15  $\mu\text{m}$  adhesive layer, polyester substrates of 50  $\mu\text{m}$ , and 175  $\mu\text{m}$  thickness [13]. The low energy 5 MeV alpha particles can easily be absorbed in the layers of 50  $\mu\text{m}$  polyester and 15  $\mu\text{m}$  adhesive, the removal of these layers allows all 5 MeV alpha particles to interact and lose their total energies in the 30  $\mu\text{m}$  thick active layer, resulting in an observed color difference.

This study aims to peel-off the Gafchromic EBT2 film to measure the absorbed dose curve of 5 MeV alpha particles. The peeled-off film was scanned to check its homogeneity. Subsequently, the peeled-off film was irradiated with 5 MeV alpha particles from  $^{241}\text{Am}$  at varying doses. After irradiation, the film was scanned using a Canon CanoScan flatbed scanner model 9000F Mark-II. Utilizing the free code software ImageJ, the red, green, and blue color channels are analyzed. Following this, the edge spread function (ESF) is determined and fitted with the error function. By differentiating the ESF, the line spread function (LSF) is obtained, then the spatial resolution could be determined as the full width at half maximum (FWHM).

## II. MATERIALS AND METHODS

In the subsequent sections, we refer to the peeled-off EBT2 Gafchromic film as P-EBT2 to investigate low-energy alpha particles (5 MeV). The Gafchromic EBT2 radiochromic film (Lot No. A06281102B) was peeled off. The peeling process, illustrated in Fig. 1, involves removing the polyester over-laminate layer (50  $\mu\text{m}$ ), the adhesive layer (15  $\mu\text{m}$ ), and the top coat layer (5  $\mu\text{m}$ ). Fig. 2(a) depicts the original structure of the Gafchromic EBT2 radiochromic film, while Fig. 2(b) shows the structure of the P-EBT2 film.

A Canon CanoScan flatbed scanner 9000F Mark-II was utilized to digitize the P-EBT2 film [14]. The Canon CanoScan was configured to a resolution of 4800 dpi, with a 48-bit RGB color scale in transmission read-out mode. The intensities of the transmitted light were measured using the scanner's software application with its default settings. Throughout all scans, the orientation of the films remained constant, with the P-EBT2 film positioned at the center of the scanner bed. Images obtained from the flatbed scanner were analyzed using the free code software ImageJ and stored in TIFF format [15].

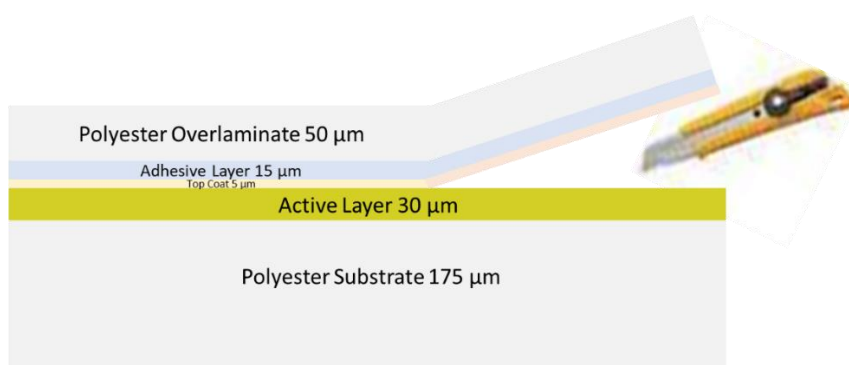


**Fig. 1.** The removal process involved peeling the polyester over-laminate layer (50  $\mu\text{m}$ ), the adhesive layer (15  $\mu\text{m}$ ), and the top coat layer (5  $\mu\text{m}$ ).

The homogeneity of the P-EBT2 Gafchromic film was examined by scanning the film and determining its plot profile and histogram. Fig. 2(c) shows the scanned image of the P-EBT2 film with an area of 10605  $\mu\text{m} \times 795 \mu\text{m}$ . All P-EBT2 Gafchromic films were found to be homogeneous, with no significant changes observed on the P-EBT2 surface, as illustrated in Fig. 2(c).

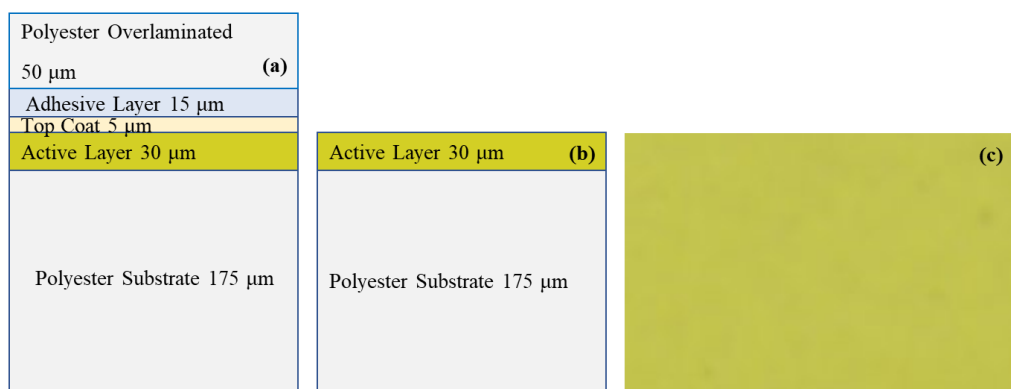


**Fig. 2.** (a) Structure of GafChromic EBT2 film. (b) The structure of the P-EBT2 film after removing the polyester layer of (50  $\mu\text{m}$ ), the adhesive layer of (15  $\mu\text{m}$ ), and the top coat layer of (5  $\mu\text{m}$ ) above the active layer of 30  $\mu\text{m}$ . (c) The image of the P-EBT2 using Canon CanoScan 9000 Mark-II flatbed scanner with an area of 10605  $\mu\text{m} \times 795 \mu\text{m}$ .

The homogeneity of the P-EBT2 film was examined by plotting the line profile and histogram of the film across the different color channels using the Canon CanoScan scanner. The image in Fig. 2(c) was analyzed, and the line profiles of the red, green, and blue channels were examined, as depicted in Fig. 3(a). This data was linearly fitted, with the fit parameters provided in Table 1. The pixel values of the red, green, and blue channel histograms of the P-EBT2 film image are shown in Fig. 3(b), with the red channel peaking at  $49839 \pm 314$ , the green channel at  $49867 \pm 330$ , and the blue channel at  $19995 \pm 538$ . Furthermore, Fig. 3(a) demonstrates that the measured line profile of the peeled-off Gafchromic EBT2 exhibits good linearity over the distance. The red channel slope (variation) is  $(-0.0095 \pm 0.0008)$  pixel value/ $\mu\text{m}$ , the green channel variation is  $(-0.011 \pm 0.0008)$  pixel value/ $\mu\text{m}$ , and the blue channel variation is  $(0.028 \pm 0.001)$  pixel value/ $\mu\text{m}$ .

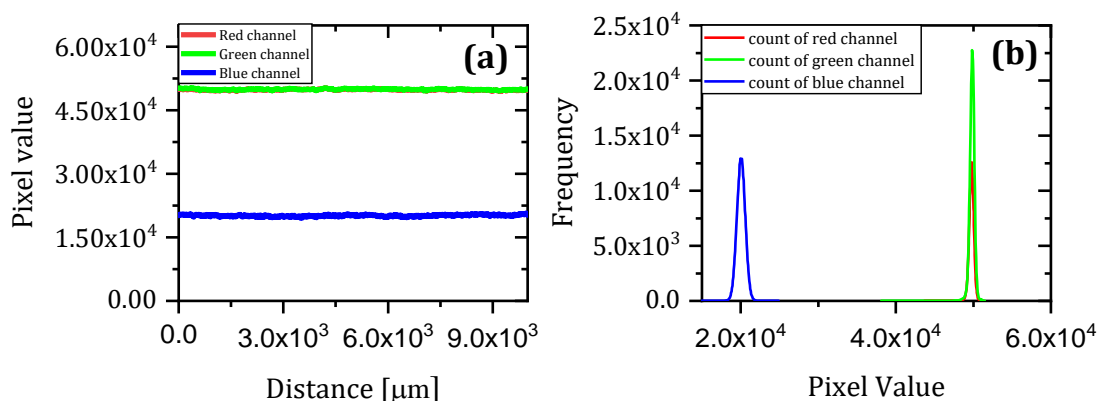


**Fig. 3.** (a) Line profile of the P-EBT2 GafChromic film for the red, green, and blue color channels, scanned with a pixel size of 5.3  $\mu\text{m} \times 5.3 \mu\text{m}$ . (b) The histogram of the P-EBT2 film of the three different color channels.

**Table 1** The fit parameters of the line profile data shown in Fig. 3 (a) of the P-EBT2 film, which was scanned using a Canon CanoScan 9000 Mark-II flatbed scanner with a pixel size of 5.3  $\mu\text{m} \times 5.3 \mu\text{m}$ .

Color channel	Mean pixel value	Intersect	Slope
Red	$49804 \pm 314$	$49854 \pm 5.4$	$-0.0095 \pm 0.0008$
Green	$49892 \pm 331$	$49955 \pm 5.5$	$-0.011 \pm 0.0008$
Blue	$20105 \pm 538$	$19953 \pm 8.7$	$0.028 \pm 0.001$

Alpha particles of energy 5.48 MeV were emitted by  $^{241}\text{Am}$  with an activity of 330 kBq. The  $^{241}\text{Am}$  radiation source is encapsulated in a precious metal foil, covered with a 3  $\mu\text{m}$  layer of gold leaf [16]. The alpha source is not in direct contact with the P-EBT2 film. Consequently, the energy of alpha particles interacting with the active layer of the P-EBT2 film is not exactly 5.48 MeV but varies depending on the distance between the source and the film, as described by the following relation [17]:

$$E(\text{MeV}) = ((R_0 - d)/0.32)^{0.667} \quad (1)$$

Here,  $R_0$  represents the range of the 5.48 MeV alpha particles in air, with a value of 4.02 cm at Normal Temperature and Pressure (NTP), and ( $d$ ) is the distance between the radiation source and the P-EBT2 film. In the current experimental setup, the value of ( $d$ ) is approximately 0.45 cm. Thus, the remaining energy of alpha particles that interact with the active layer of the P-EBT2 film can be measured using the previous formula, resulting in an energy of 5 MeV.

The accompanying Fig. 4. illustrates the experimental setup, featuring a razor blade, the P-EBT2 film, and alpha particles with an actual energy of 5 MeV upon reaching the active layer of the P-EBT2 film. This setup is used to create the edge spread function (ESF).

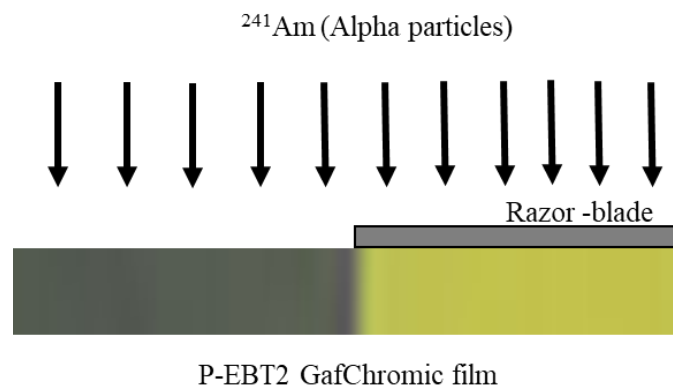


**Fig. 4.** The experimental setup of irradiating the P-EBT2 film, by using a razor blade kept in contact with the active layer of the P-EBT2, and alpha particles of 5 MeV for various doses to produce two distinct halves and produce the edge spread function (ESF).

The flux of alpha particles that interacted and absorbed in the active layer of the P-EBT2 film was calculated by the following relation:

$$\phi = (A/4\pi d^2) * t \quad (2)$$

Here,  $A$  represents the activity of the radioactive source  $^{241}\text{Am}$ ,  $d$  is the distance between the radioactive source and the P-EBT2 film measured in centimeters (cm), and  $t$  is the exposure time to alpha particles measured in seconds.

As previously described, the active layer of the EBT2 film has a thickness of 30  $\mu\text{m}$ , where the range of 5 MeV alpha particles is less than this 30  $\mu\text{m}$  thickness, resulting in their complete absorption within the active layer. The absorbed dose in the active layer of the P-EBT2 film, measured in Gray (Gy), can be calculated using the following relation [18]:

$$D (\text{Gy}) = 1.6 \times 10^{-10} \cdot \frac{\text{LET} \left( \frac{\text{MeV}}{\text{cm}} \right) \cdot \phi \left( \frac{\text{Alphas}}{\text{cm}^2} \right)}{\rho \left( \frac{\text{gm}}{\text{cm}^3} \right)} \quad (3)$$

Here, LET represents the linear energy transfer of alpha particles in the active layer of the P-EBT2 film, obtained from the SRIM/TRIM program with a value of 1031 MeV/cm [19], and  $\rho$  is the mass density of the material through which the radiation passes (active layer) with a value of 1.2  $\text{g}/\text{cm}^3$ . The constant factor  $1.6 \times 10^{-10}$  converts energy from the LET in MeV/cm to Gray (Gy).

An alpha particle source with an energy of 5 MeV was used to irradiate four films, each for different exposure times. These times correspond to fluence [alphas/cm<sup>2</sup>] of alpha particles emitted from the <sup>241</sup>Am source and absorbed doses [Gy] displayed in Table 2. After irradiation, the P-EBT2 films were scanned using a Canon CanoScan 9000F Mark-II, then analyzed with the free code software ImageJ and saved in TIFF format. Images of the dark areas (only the irradiation part) for each dose of the P-EBT2 films with an area of 265 µm × 265 µm are shown in Fig. 5.

**Table 2** The fluence [alphas/cm<sup>2</sup>] of alpha particles emitted from <sup>241</sup>Am source, and the corresponding absorbed dose, measured in [Gy] of 5 MeV alpha.

Fluence [alphas/cm <sup>2</sup> ]	Absorbed Dose [Gy]
$7.57 \times 10^7$	10.41
$1.51 \times 10^8$	20.75
$3.78 \times 10^8$	51.97
$5.29 \times 10^8$	72.72



**Fig. 5.** Images of the dark areas of the P-EBT2 films irradiated with an alpha particle of energy 5 MeV for various doses were scanned using the Canon CanoScan flatbed scanner 9000F Mark-II with an area of 265 µm × 265 µm.

### III. RESULTS AND DISCUSSION

#### III.1 Characterization of the scanned images

In principle, two-dimensional dosimetry in both heavy ion radiotherapy and alpha-emitter therapy requires high spatial and dose resolution [3, 5]. The spatial resolution of the P-EBT2 film is influenced by both the film's structure and the type of radiation. However, since the color channels of radiochromic films respond differently to absorbed doses, it is important to conduct an in-depth investigation of the spatial resolution dependence on the red, green, and blue channels, as well as weighted and unweighted gray images [20, 21]. The film was scanned using a Canon CanoScan 9000F Mark-II flatbed scanner in transmission read-out mode at a pixel size of 5.3 µm × 5.3 µm and a color depth of 2<sup>16</sup> per channel, as illustrated in Fig. 6.

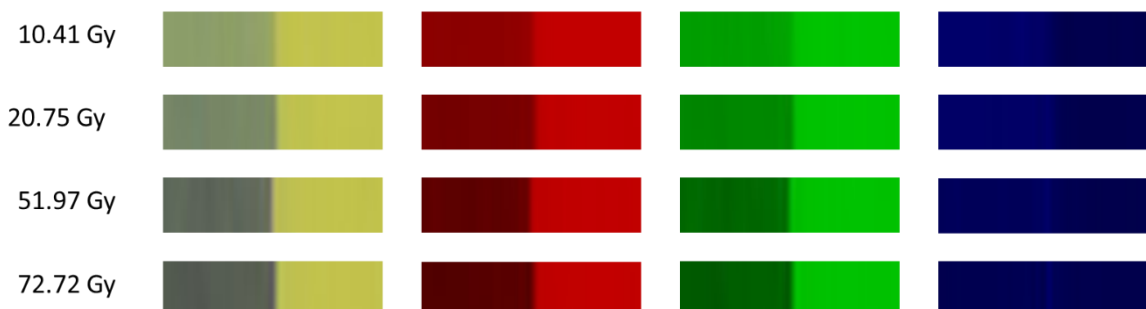


**Fig. 6.** The RGB images and the individual red, green, and blue channels of the P-EBT2 film, with an image area of  $795 \mu\text{m} \times 26.5 \mu\text{m}$ , exposed to different doses of 5 MeV alpha particles. The left part represents the irradiated part, while the right part remains unirradiated. The images were scanned using a resolution of  $5.3 \mu\text{m} \times 5.3 \mu\text{m}$  per pixel.

For quantitative analysis of the images shown in Fig. 6, the relationship between pixel value and the dose of 5 MeV alpha particles is evaluated. Similar to dosimetry for gamma rays and electron beams, exposure to 5 MeV alpha particles results in increased film blackness, which corresponds to a reduction in pixel values. The red, green, and blue channels can be processed in RGB, as well as the weighted and unweighted gray images. The weighted and unweighted gray images of the P-EBT2 film are calculated using the following relationship:

$$\text{UnWeighted grey image} = \frac{R+G+B}{3} \quad (4)$$

$$\text{Weighted grey image} = 0.299R + 0.587G + 0.114B. \quad (5)$$

As exposure time increases, the absorbed dose in the active layer increases, leading to greater film darkness and a corresponding decrease in pixel values [6]. Fig. 7 demonstrates that with increasing the absorbed dose, the pixel values decrease until saturation is reached.

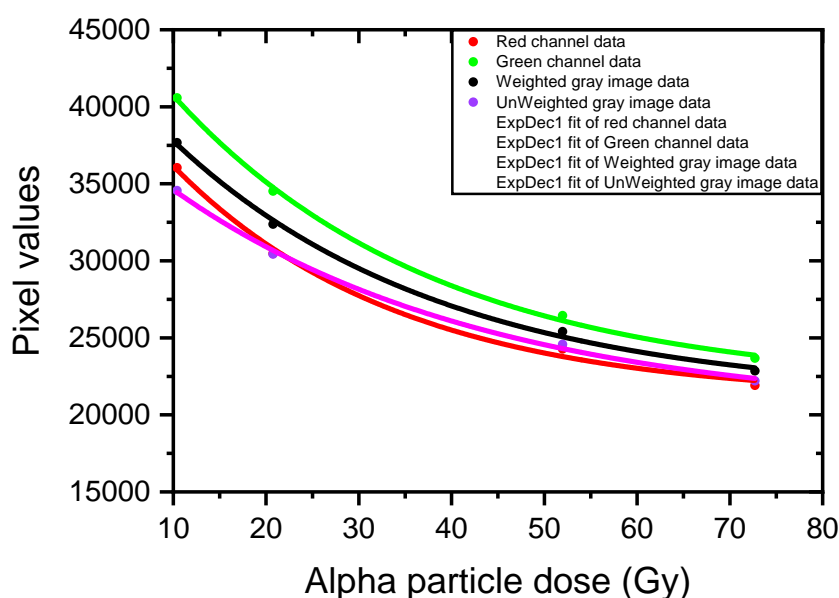


**Fig. 7.** The variation in pixel values across different doses and color channels of the P-EBT2 samples, irradiated with 5 MeV alpha particles, was digitized using the Canon CanoScan 9000F Mark-II flatbed scanner.

The data presented in Fig. 7 were fitted using an exponential decay function as follows:

$$PV(D\alpha) = PV_0 + a_1 \text{Exp}(-k * D\alpha) \quad (6)$$

Where  $PV_0$  represents the intensity when the dose is very large (the intensity at saturation),  $a_1$  represents the initial change in intensity,  $k$  is a constant that determines the rate of decay, and Table 3 represents the fitting parameters.

For the red channel, the initial pixel value ( $PV_0$ ) and the decay rate are  $21045 \pm 1304$  and  $0.040 \pm 0.010$ . For the green channel, the initial pixel value ( $PV_0$ ) and decay rate are  $21780 \pm 1183$  and  $0.035 \pm 0.005$ . The weighted gray image has values of  $21111 \pm 1293$  for the ( $PV_0$ ) and  $0.034 \pm 0.007$  for the decay rate, and the unweighted gray image has  $20038 \pm 1473$  for the ( $PV_0$ ) and  $0.029 \pm 0.006$  for the decay rate.

**Table 3** The fitting parameters of the pixel values (PV) for the red and green channels, as well as the weighted and unweighted gray images, as a function of 5 MeV alpha particle doses in the peeled-off Gafchromic™ EBT2 film, using the exponential decay function.

Color channel	$PV_o$	$a_1$	$k(\text{Gy}^{-1})$	$R^2$
Red	$21045 \pm 1304$	$22696 \pm 1819$	$0.040 \pm 0.010$	0.996
Green	$21780 \pm 1183$	$26934 \pm 1024$	$0.035 \pm 0.005$	0.998
Weighted gray image	$21111 \pm 1293$	$23498 \pm 1041$	$0.034 \pm 0.007$	0.998
Unweighted gray image	$20038 \pm 1473$	$19534 \pm 881$	$0.029 \pm 0.006$	0.998

Another important relationship between the contrast of the P-EBT2 film and the variety of doses was studied. As the doses increase, the contrast (visibility) also increases, as depicted in Fig. 8. The values of contrast can be obtained from the following relationship:

$$C(\%) = \left(1 - \frac{I(\text{exp})}{I(\text{unexp})}\right) * 100 \quad (7)$$

Here,  $C$  is the contrast in percentage,  $I(\text{exp})$  is the pixel value of the irradiated film, and  $I(\text{unexp})$  is the pixel value of the unirradiated film.

The data presented in Fig. 8 were fitted using an exponential growth function as follows:

$$C(D_\alpha) = C_m + A_1 \text{Exp}(-A_2 * D_\alpha) \quad (8)$$

where  $C_m$  represents the contrast when the dose is very large (the contrast at saturation),  $A_1$  represents the initial changes in contrast, and  $A_2$  is a constant, which determines the rate of growth, and  $D_\alpha$  is the dose of alpha particles, and **Table 4** represents the fitting parameters of that equation.

**Table 4** The fitting parameters of the contrast ( $C$ ) for the red and green channels, as well as the weighted and unweighted gray images

Color channel	$C_m$	$A_1$	$A_2$	$R^2$
Red	$57.8 \pm 2.6$	$-45.5 \pm 3.6$	$0.04 \pm 0.01$	0.98
Green	$56.3 \pm 2.4$	$-54 \pm 2.1$	$0.035 \pm 0.005$	0.99
Weighted gray image	$57.6 \pm 2.6$	$-47.1 \pm 2.1$	$0.034 \pm 0.007$	0.99
Unweighted gray image	$59.8 \pm 2.9$	$-39.2 \pm 1.8$	$0.029 \pm 0.006$	0.99



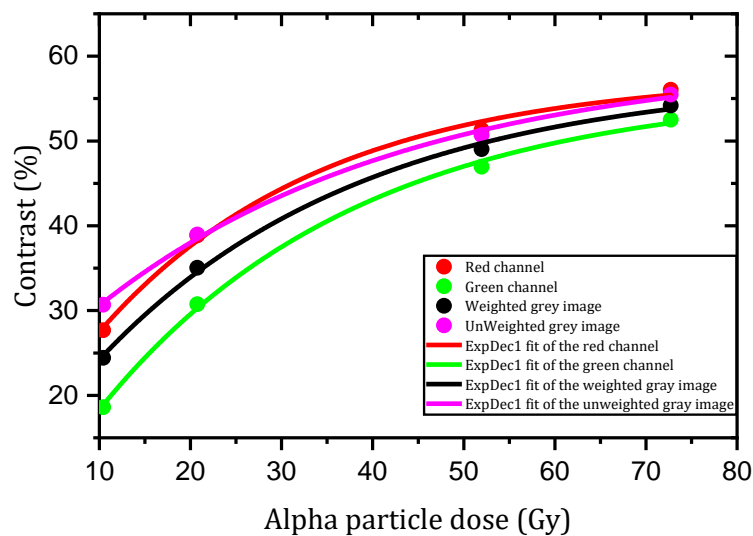


**Fig. 8.** The contrast in percentage (%) versus the doses of alpha particle in (Gy) of the red and green channels, as well as the weighted and unweighted gray images.

### III.2 Measuring the ESF and LSF

#### III.2.1 The edge spread function (ESF)

The edge spread function (ESF) was generated using a razor blade held in close contact with the active layer of the P-EBT2 film. The 5 MeV alpha particles were incident normally at different doses, resulting in two distinct regions: one brighter (unexposed) and the other darker (exposed). Fig. 9 shows the dependence of the experimental edge spread on the individual red, green, and blue channels, as well as the weighted and unweighted gray images, at 5 MeV alpha particle doses of (a) 10.41 Gy, (b) 20.75 Gy, (c) 51.97 Gy, and (d) 72.72 Gy. The measured edge spread data can be fitted using various functions, but the error function is the most commonly applied:

$$R(x) = b_1 + b_2 \cdot \text{Erf} \left( \frac{x-x_0}{b_3} \right). \quad (9)$$

Here,  $b_1$  represents the minimum value of the response function  $R(x)$ ,  $b_2$  denotes the strength or magnitude of the transition from the minimum to the maximum value,  $x_0$  compensates for the lateral shift of the ESF to any arbitrary location on the x-axis, and  $b_3$  is the scaling factor associated with the edge width, which correlates with the spatial resolution.

From Fig. 9, it can be observed that the red and green channels, as well as the weighted and unweighted gray images, consistently exhibit a step transition between exposed and unexposed regions, characterized by a sharp rise in pixel values. This transition indicates a well-defined edge spread. In contrast, the blue channel displays an inverted or irregular response, where the exposed area appears unexpectedly brighter or has less contrast than the unexposed area, indicating limited sensitivity to alpha particle exposure. Due to this abnormal behavior of the blue channel, the data from that channel cannot be fitted with the error function.



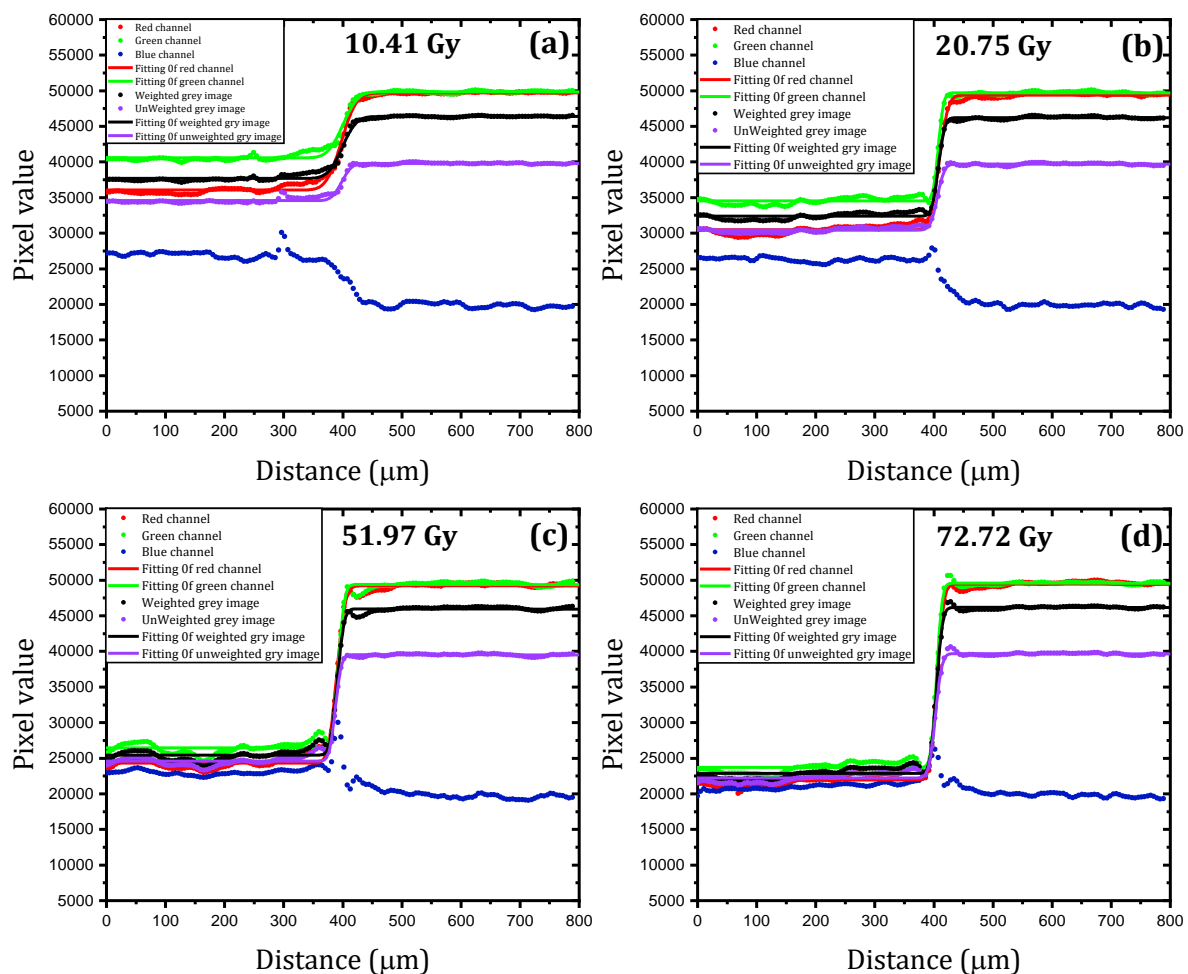


**Fig. 9.** The experimental edge spread function of the weighted and unweighted gray images and the associated single red, green, and blue channel dependence on the 5 MeV alpha particle doses of the P-EBT2 film. The data points correspond to the doses: (a) 10.41 Gy, (b) 20.75 Gy, (c) 51.97 Gy, and (d) 72.72 Gy. The solid line is the data fitting using the error function.

### III.2.2 The line spread function (LSF)

The error function, which represents the integral of the Gaussian function and vice versa, is commonly used to fit the edge spread function (ESF). Differentiating the error function in Eq. 9 with respect to distance ( $x$ ) yields the line spread function (LSF), as follows.:

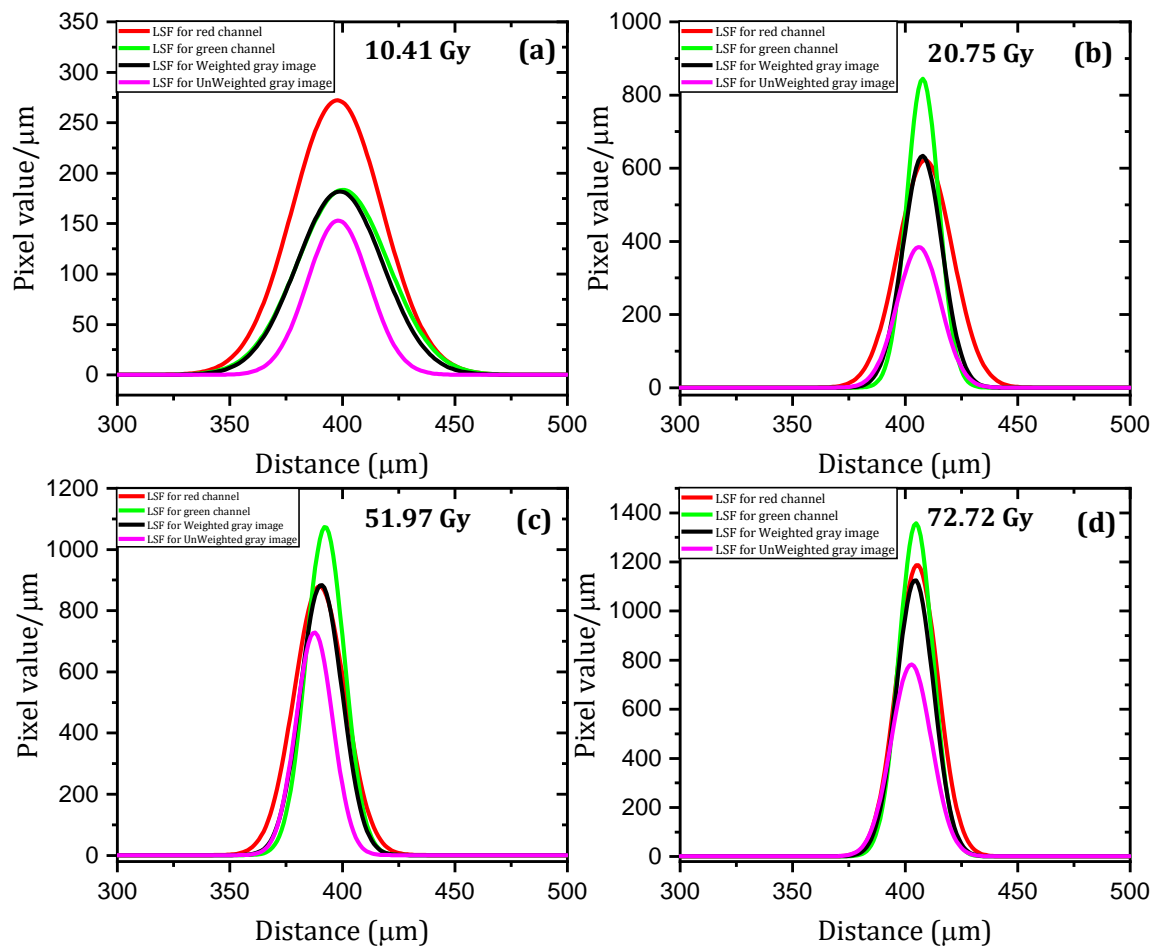
$$\frac{dR(x)}{dx} = \frac{d(b_1 + b_2 \cdot \text{Erf}(\frac{x-x_0}{b_3})}{dx} = \frac{2 b_2 e^{-\frac{(x-x_0)^2}{b_3^2}}}{b_3 \sqrt{\pi}} \quad (10)$$

Fig. 10. shows the line spread functions for the different color channels, red and green channels, as well as weighted and unweighted gray images dependence on the 5 MeV alpha particle doses of (a) 10.41 Gy, (b) 20.75 Gy, (c) 51.97 Gy, and (d) 72.72 Gy. The blue channel is excluded because it can't be fitted with the error function. Table 5 shows the spatial resolution for the different color channels, red and green channels, as well as weighted and unweighted gray images at different doses in terms of the full width at half maximum (FWHM).

**Table 5** The spatial resolution in terms of the full width at half maximum (FWHM) for the different color channels red and green channels, as well as weighted and unweighted gray images of the P-EBT2 film exposed to different doses of 5 MeV alpha particles

Absorbed Dose [Gy]	Red channel [ $\mu\text{m}$ ]	Green channel [ $\mu\text{m}$ ]	Weighted gray image [ $\mu\text{m}$ ]	Unweighted gray image [ $\mu\text{m}$ ]
<b>10.41</b>	$47.1 \pm 9$	$47.5 \pm 8.7$	$45 \pm 1$	$32.2 \pm 2.8$
<b>20.75</b>	$28.5 \pm 4$	$16.8 \pm 2$	$20.5 \pm 1.1$	$22.6 \pm 8.1$
<b>51.97</b>	$26.6 \pm 5$	$20.1 \pm 1.2$	$21.8 \pm 9.1$	$19.2 \pm 1.3$
<b>72.72</b>	$21.7 \pm 9.1$	$17.9 \pm 1.6$	$19.4 \pm 1.3$	$21 \pm 1$

At different doses, the average values of the spatial resolution are  $31 \pm 6.7 \mu\text{m}$ ,  $25.6 \pm 3.4 \mu\text{m}$ ,  $26.7 \pm 3.1 \mu\text{m}$ , and  $23.8 \pm 3.3 \mu\text{m}$ , for the red and green channels, as well as the weighted, and unweighted gray images, respectively. Showing that the unweighted gray image and the green channel have the highest spatial resolution compared to the other channels.



**Fig. 10.** The line spread functions of the weighted and unweighted gray images and the associated single red and green channel dependence on the 5 MeV alpha particle doses of (a) 10.41 Gy, (b) 20.75 Gy, (c) 51.97 Gy, and (d) 72.72 Gy.

#### IV. Conclusion

The relationship between spatial resolution and contrast of peeled-off EBT2 radiochromic film irradiated with monoenergetic alpha particles across various color channels has been investigated. The peeled-off Gafchromic

EBT2 films were irradiated by 5 MeV alpha particles from  $^{241}\text{Am}$  with multiple doses. To produce two distinct halves (edges), a razor blade was kept in close contact with the active layer of the film. The pixel values decrease with the increase in the absorbed dose. Also, it was found that the contrast increases with the increase in the absorbed dose values for all the color channels. Using the error function, the measured edge spread function (ESF) for different color channels as well as weighted and unweighted gray images, were fitted and thereafter differentiated to produce the line spread function (LSF). The red and green channels and the weighted and unweighted gray images consistently exhibit a step transition between exposed and unexposed regions, characterized by a sharp rise in pixel values. This transition indicates a well-defined edge spread. In contrast, the blue channel displays an inverted or irregular response, where the exposed area appears unexpectedly brighter or has less contrast than the unexposed area, indicating limited sensitivity to alpha particle exposure. The average spatial resolution expressed as the full width at half maximum (FWHM), was found to be  $31 \pm 6.7 \mu\text{m}$ ,  $25.6 \pm 3.4 \mu\text{m}$ ,  $26.7 \pm 3.1 \mu\text{m}$ , and  $23.8 \pm 3.3 \mu\text{m}$ , for the red and green channels, as well as the weighted, and unweighted gray images, respectively. These results show that the unweighted gray image and the green channel provide the highest spatial resolution.

## V. References

- Williams, M., et al., *Radiochromic Film Dosimetry and its Applications in Radiotherapy*. 2011. p. 75-99.
- Devic, S., N. Tomic, and D. Lewis, *Reference radiochromic film dosimetry: Review of technical aspects*. Phys Med, 2016. **32**(4): p. 541-56.
- Devic, S., *Radiochromic film dosimetry: past, present, and future*. Phys Med, 2011. **27**(3): p. 122-34.
- Hall, A.V., et al., *Alkali Metal Salts of 10,12-Pentacosadiynoic Acid and Their Dosimetry Applications*. Cryst Growth Des, 2021. **21**(4): p. 2416-2422.
- Xing, L., et al., *Overview of image-guided radiation therapy*. Medical Dosimetry, 2006. **31**(2): p. 91-112.
- Das, I.J., *Radiochromic film: role and applications in radiation dosimetry*. 2017: CRC Press.
- Soares, C.G., *Radiochromic film dosimetry*. Radiation measurements, 2006. **41**: p. S100-S116.
- Santos, T., T. Ventura, and M.d.C. Lopes, *A review on radiochromic film dosimetry for dose verification in high energy photon beams*. Radiation Physics and Chemistry, 2021. **179**.
- Butson, M.J., et al., *Radiochromic film for medical radiation dosimetry*. Materials Science and Engineering: R: Reports, 2003. **41**(3-5): p. 61-120.
- Casolaro, P., *Radiochromic Films for the Two-Dimensional Dose Distribution Assessment*. Applied Sciences, 2021. **11**(5).
- Grilj, V. and D. Brenner, *LET dependent response of GafChromic films investigated with MeV ion beams*. Physics in Medicine & Biology, 2018. **63**(24): p. 245021.
- Butson, M.J., T. Cheung, and P.K. Yu, *Absorption spectra variations of EBT radiochromic film from radiation exposure*. Physics in Medicine & Biology, 2005. **50**(13): p. N135.
- El-Naggar, H.I., et al., *On the registration of low energy alpha particle with modified GafChromic EBT2 radiochromic film*. Radiation Physics and Chemistry, 2022. **191**.
- Canon, *Canon*, in *Canon CanoScan 9000F Mark II* 2023.
- ImageJ, *ImageJ*, in *ImageJ*. 2023.
- LEYBOLD, *LEYBOLD*, in *LEYBOLD*. 2023.
- Hassib, G.M. and H.A. Amer, *Optimization of electrochemical track etching for alpha particle spectrometry*. Nuclear Tracks and Radiation Measurements, 1993. **22**(1): p. 121-124.
- Basset, A., et al., *Investigation of energy dependance for EBT3 response to irradiation with alpha beams*. Nuclear Instruments and Methods in Physics Research Section B: Beam Interactions with Materials and Atoms, 2019. **454**: p. 56-60.
- Ziegler, J.F. and J.P. Biersack, *The stopping and range of ions in matter*, in *Treatise on heavy-ion science: volume 6: astrophysics, chemistry, and condensed matter*. 1985, Springer. p. 93-129.
- Al-Sayed, A., et al., *On the color channel's effect on the dose-response of Gafchromic EBT2 and EBT3 radiochromic films to 6 MeV electron beam*. Radiation Physics and Chemistry, 2024. **218**: p. 111565.
- Mohamed, A., et al., *Evaluation of the spatial resolution of the peeled-off Gafchromic EBT2 film irradiated with different doses of low-energy alpha particles from  $^{241}\text{Am}$* . Physica Scripta, 2025. **100**(3): p. 035304.